Angewandte Chemie
Eine Zeitschrift der Gesellschaft Deutscher Chemiker

Supporting Information

The Effect of Surface Site Ensembles on the Activity and Selectivity of Ethanol Electrooxidation by Octahedral PtNiRh Nanoparticles

*Nina Erini, Vera Beermann, Martin Gocyla, Manuel Gliech, Marc Heggen, Rafal E. Dunin-Borkowski, and Peter Strasser**

ange_201702332_sm_miscellaneous_information.pdf

Supporting Information:

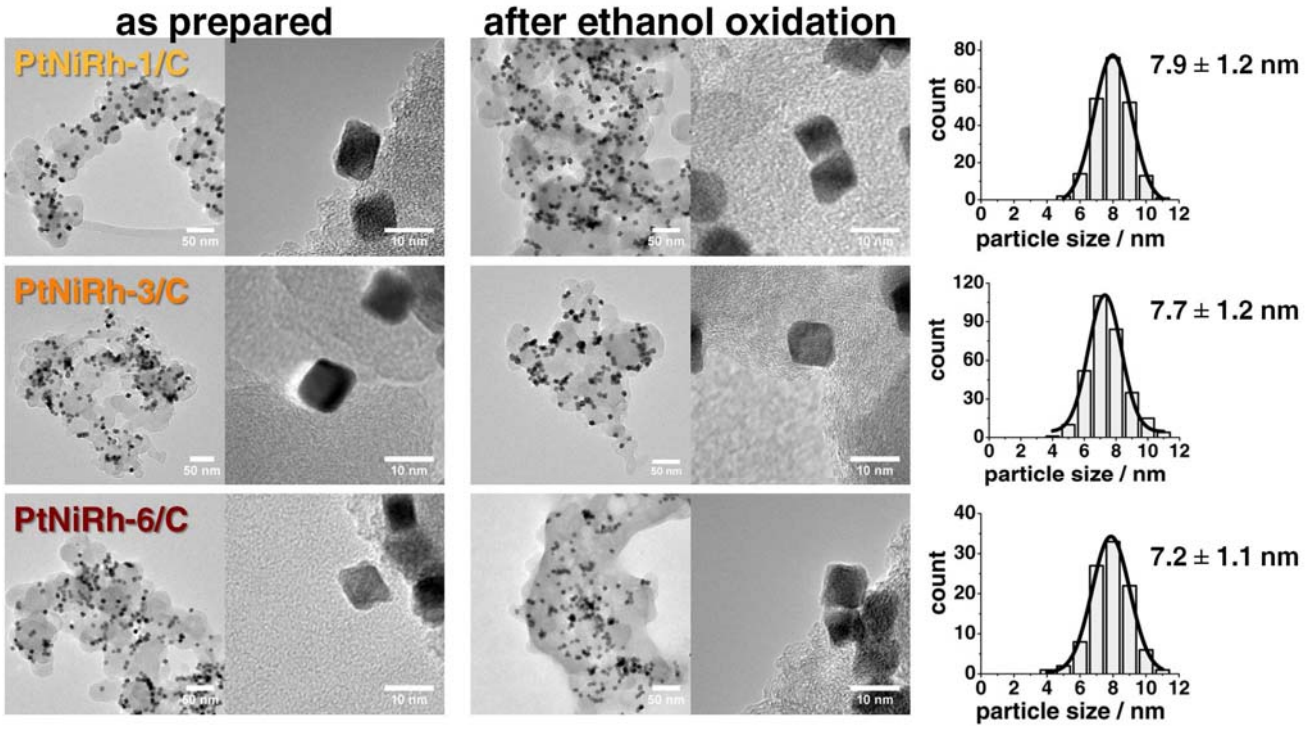

Figure S 1: Edge length distribution and lattice spacing of the *$Pt_3Ni_1Rh_x$-oct/C* electrocatalysts. TEM micrographs as prepared (left), after one scan in 0.5 M EtOH in 0.1 M KOH (middle) and edge length distribution histograms (right) of *PtNiRh-oct/C* electrocatalysts.

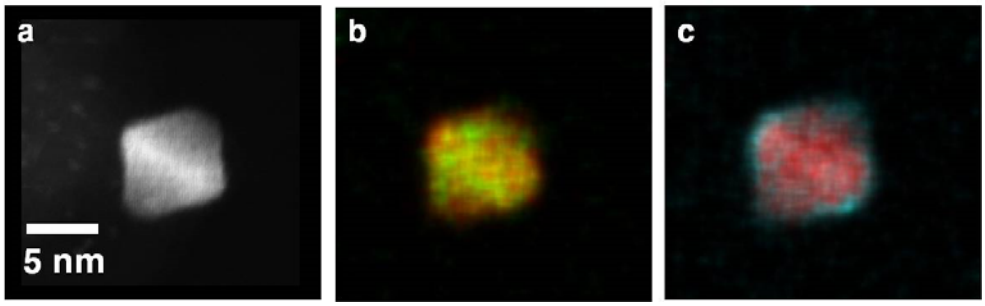

Figure S 2: **Atomic-scale composition profile analysis of *PtNiRh-6/C* octahedral nanoparticles.** HAADF STEM image (**a**) and EDX composition map analysis **(b-c)** after the first EOR scan of a *PtNiRh-6/C* octahedral nanoparticle (6.5 nm). (**b**) EDX composition map showing the distribution of Pt (red) and Ni (green) and (**c**) Pt (red) and Rh (blue), respectively.

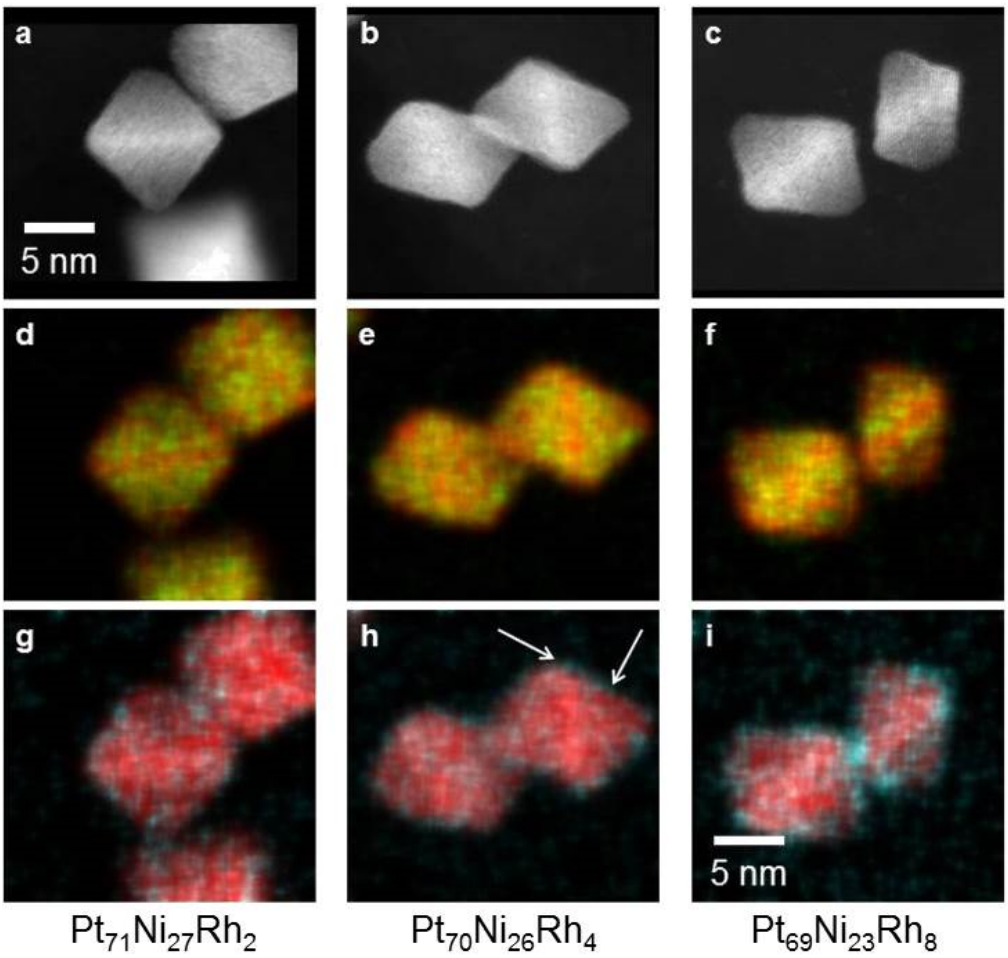

Figure S 3: Atomic-scale Z-contrast STEM images and composition profile analysis of as-prepared *$Pt_3Ni_1Rh_x$-oct/C* octahedral nanoparticles. HAADF STEM images (**a-c**) and EDX composition map analysis (**d-i**) of *PtNiRh-1/C* (**a,d,g**), *PtNiRh-3/C* (**b,e,h**) and *PtNiRh-6/C* (**c,f,i**) octahedral nanoparticles oriented close to ⟨110⟩. **(d-f)** EDX composition map showing the distribution of Pt (red) and Ni (green) and (**g-i**) Pt (red) and Rh (blue), respectively.

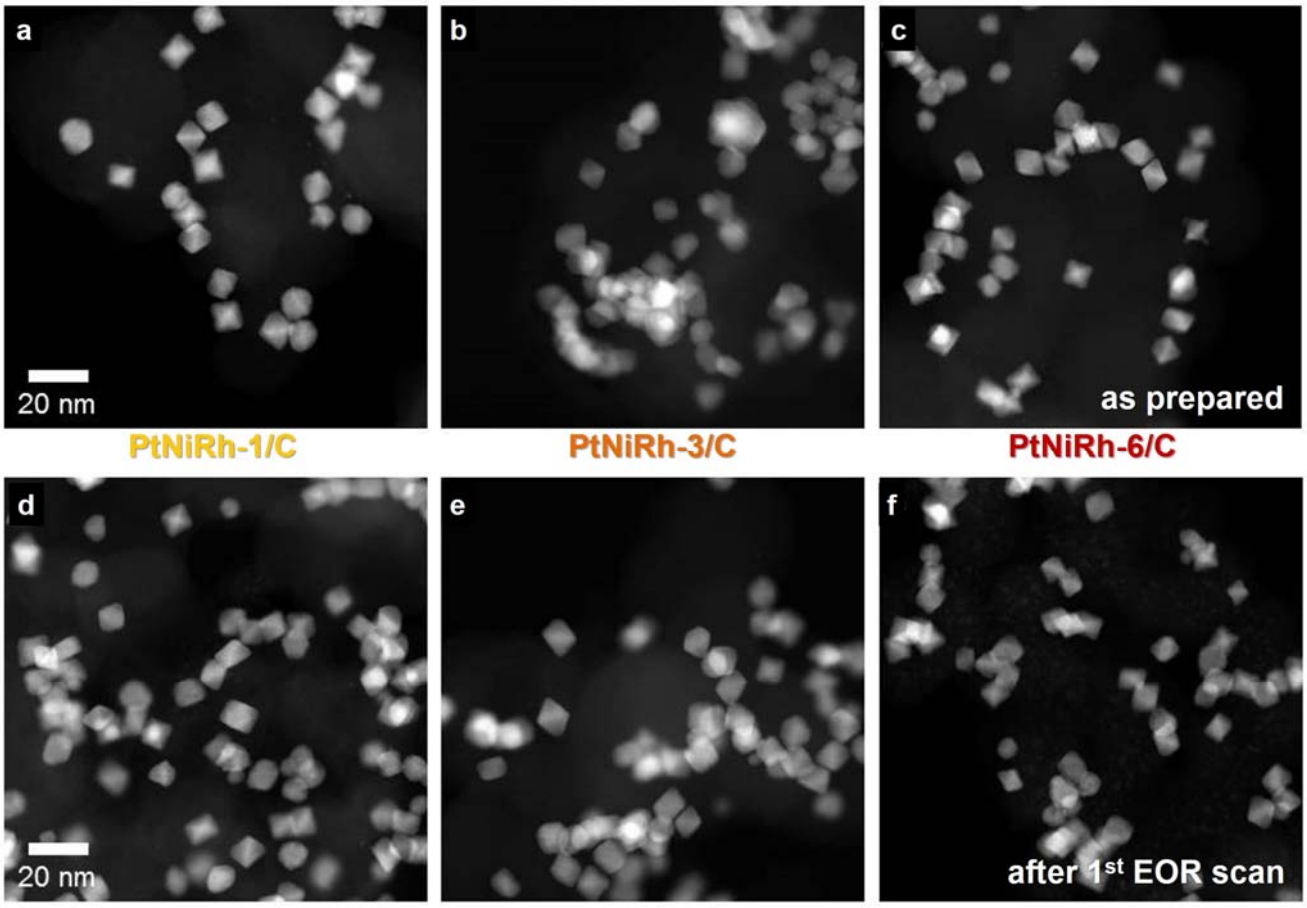

Figure S 4: **Comparison of HAADF STEM images, as prepared and after the first EOR scan on *$Pt_3Ni_1Rh_x$-oct/C* octahedral nanoparticles.** HAADF STEM images before (**a-c**) and after (**d-f**) the first EOR scan for *PtNiRh-1/C* (**a,d**), *PtNiRh-3/C* **(b,e)** and *PtNiRh-6/C* **(c,f,)** octahedral nanoparticles.

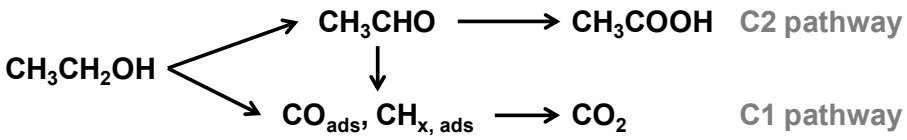

Figure S 5: Intermediates and products occurring on the anodic side of the direct ethanol fuel cell. Schematic representation of the dual pathway mechanism for the electrooxidation of ethanol. Adapted from Lai et al[1] and Christensen et al.[2]

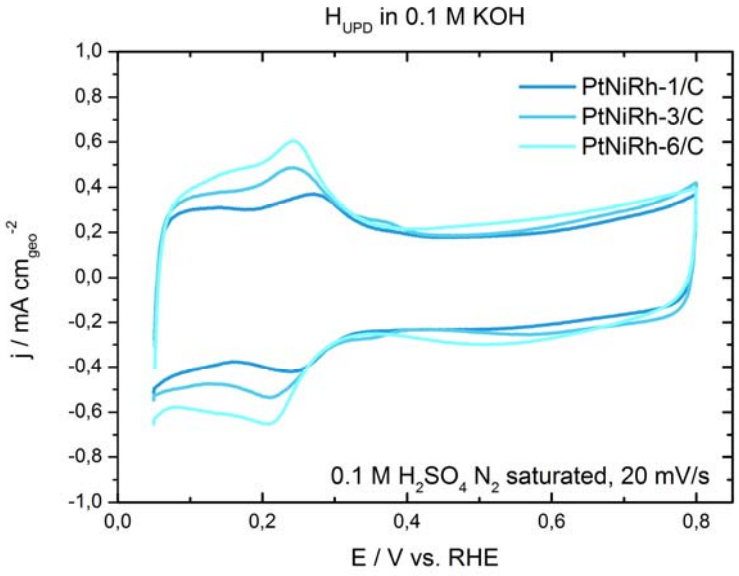

Figure S 6: First polarization curves of PtNiRh-X/C in pure 0.1 M KOH. Current densities are normalized by the geometric are (0.196 cm^2). Scan rate is v = 20 mVs^{-1}.

Table S 1: Size, molar composition and metal weight loading of supported *PtNiRh-oct/C* electrocatalysts.

Catalysts	**Atomic ratio (Pt:Ni:Rh)**	**Total metal loading wt%**	**Average particle size (nm)**	
			as prepared	after 1st EOR scan
1) PtNiRh-1/C	71:28:1	25	8.0 ± 1.0	7.9 ± 1.2
2) PtNiRh-3/C	77:20:3	31	7.9 ± 1.2	7.7 ± 1.3
3) PtNiRh-6/C	67:27:6	21	7.3 ± 1.2	7.2 ± 1.1

Table S 2: Comparison of experimental 2θ values with theoretical 2θ values for all *PtNiRh-oct/C* electrocatalysts derived from Vegard's law for fcc phases.[3]

Catalyst	(hkl)	d_{theo} [A]	$2\theta_{theo}$	$2\theta_{exp}$
1) PtNiRh-1/C	(111)	2.200	41.0	40.7
	(200)	1.905	47.7	47.4
	(220)	1.347	69.8	69.3
2) PtNiRh-3/C	(111)	2.217	40.7	40.5
	(200)	1.920	47.3	47.2
	(220)	1.358	69.1	69.9
3) PtNiRh-6/C	(111)	2.199	41.0	40.7
	(200)	1.904	47.7	47.5
	(220)	1.346	69.8	69.3

Table S 3: Electrochemical EOR activity of *PtNiRh-oct/C* catalysts: electrochemical surface area (ECSA), mean values with standard derivation of current density at 0.45 V vs. RHE and 0.80 V vs. RHE during voltammetric scans, and current density at constant 0.45 V vs. RHE after 300 s.

Catalyst	$ECSA_{Hupd}$	j @ 0.45V	j @ 0.80V	j @ 0.45V@300s
	$m^2\ g_{Pt}^{-1}$	mA cm_{ECSA}^{-2} μg_{Pt}	mA cm_{ECSA}^{-2} μg_{Pt}	mA cm_{ECSA}^{-2} μg_{Pt}
1) PtNiRh-1/C	19.6±0.8	1.0 ± 0.2	12.0 ± 0.2	0.21
2) PtNiRh-3/C	24.0±0.2	1.4 ±0 .2	13.6 ± 0.9	0.23
3) PtNiRh-6/C	31.3±1.6	0.8 ± 0.1	6.9 ± 0.1	0.12

Experimental Details

Synthesis of *PtNiRh-oct/C*: Platinum(II)acetylacetonate ($Pt(acac)_2$, Pt 48% min.), nickel(II)acetylacetonate ($Ni(acac)_2$, 95.0 %), tungsten hexacarbonyl ($W(CO)_6$, 97.0 %) and oleic acid (OAc, 90 %) were obtained from Alfa Aesar; rhodium(III)acetylacetonate ($Rh(acac)_3$, 97.0 %), oleylamine (OAm, 70.0 %) and acetic acid (HAc, ≥ 99.9 %) were obtained from Sigma Aldrich; dibenzylether (Bn_2O, 98.0 %) was obtained from Fluka. All chemicals were used as received. In order to prepare *Pt-Ni-Rh* octahedral nanoparticles $Pt(acac)_2$ (0.102 mmol), $Ni(acac)_2$ (0.234 mmol), $Rh(acac)_3$ (0.003 mmol, 0.005 mmol, 0.012 mmol), OAm (12 mL) and OAc (8 mL) were added into a 100 ml three-neck-flask under reflux. The reaction mixture was stirred for 5 minutes under nitrogen atmosphere at 60 °C, followed by raising the temperature to 130 °C. At this temperature, nitrogen purging was stopped, $W(CO)_6$ (0.389 mmol) was added rapidly and the reaction mixture was heated to 230 °C and then stirred for 40 minutes. Then, the reaction mixture was cooled down to room temperature and toluene (10 mL) and ethanol (30 ml) were added to it. The supernatant was removed by centrifugation (7800 rpm for 5 min) and dispersed in toluene (20 mL). The dispersion was added to a dispersion of Vulcan XC 72R (0.04 g) in toluene (20 mL) and sonicated for 1 h. Ethanol (10 mL) was then added and the Pt-Rh-Ni/C catalyst was centrifuged (7800 rpm for 10 min). The resulting particles were added to acetic acid (40 mL) and refluxed for 30 min at 60 °C. After the mixture was cooled, the particles were washed with ethanol (30 mL) three times and dried for 12 h in air.

Electrochemical measurements: Linear sweep voltammograms (LSVs) recorded in ethanol containing electrolyte (Figure 2a, b) revealed high activity towards the EOR for all of the $Pt_3Ni_1Rh_x$*-oct/C* electrocatalysts. Measurements of the reduction charge of hydrogen under potential deposition (H_{UPD}) from cyclic voltammograms (CVs) in pure electrolyte were used to estimate the electrochemically active surface area (ECSA) values for the three catalysts based on the charge density for the formation of a fully covered Pt-H monolayer (210 µC/cm²).[4] ECSA values are highest for *PtNiRh-6/C* with 31.3 m² g_{Pt}^{-1}, followed by *PtNiRh-3/C* with 24.0 m² g_{Pt}^{-1} and lowest for *PtNiRh-1/C* with 19.6 m² g_{Pt}^{-1}.

Polished glassy carbon working electrodes were coated with 10 µl catalyst ink (4 mg electrocatalyst powder; 2.5 mL of ultrapure water; 0.5 mL isopropanol; 15 µL of 5 wt. % Nafion solution) and measured with a Biologic SP 150 potentiostat in an electrochemical glass cell with Pt wire as counter and a saturated SCE (in KOH) as a reference electrode. The electrolyte was freshly made and purged with nitrogen prior to and during experiments. Current densities were normalized by ECSA and the amount of Platinum present on the electrode surface. The characterization and electrochemical testing protocol for *PtRhNi-oct/C* has been described in detail elsewhere.[5]

Scanning transmission electron microscopy (STEM) was performed using a FEI Titan 80-200 ("ChemiSTEM") electron microscope, equipped with a C_s-probe corrector (CEOS GmbH) and a high-angle annular dark field (HAADF) detector. The microscope was operated at 200 kV. In order to

achieve “Z-Contrast” conditions, a probe semi-angle of 25 mrad and an inner collection semi-angle of the detector of 88 mrad were used. Compositional maps were obtained with energy-dispersive X-ray spectroscopy (EDX) using four large-solid-angle symmetrical Si drift detectors. For EDX analysis, Pt L, Ni K and Rh L peaks were used. The 1σ statistical error in the EDX quantification of ± 2 at. %, is dominated by the counting statistics. For all samples at least 10 high resolution EDX maps of different nanoparticles were obtained.

Cu K_α X-ray diffraction (XRD) patterns were collected using a D8 Advance diffractometer (Bruker) equipped with a Lynx Eye Detector and KFL Cu 2K X-ray tube. The diffraction patterns were collected over a 20–80° 2θ range with a step size of 0.05°, dwelling for 10 s at every step. The XRD patterns were analyzed using the MDI Jade 8 software package. Bragg reflection positions were compared with reference XRD patterns (PDF data files, International Center for Diffraction Data). Carbon features were taken out by background subtraction

***In situ* ATR FTIR spectroscopy** was used to investigate the IR bands of adsorbed species on the catalyst surface under potential control. Our modified attenuated total reflection (ATR) FTIR cell setup allows the investigation of supported nanoparticle ink films almost identical with standard rotating disc electrode films. The ink solution of supported electrocatalysts is deposited directly onto the ATR prism, avoiding intensity loss due to the lack of a sputtered layer of a conducting material such as Au. The electrochemical connection is made via a carbon cloth material that provides a reservoir of electrolyte over the catalyst, minimizing mass transport limitations and polarization effects, which are common problems of external reflection thin film configurations (Figure S8). The spectra were collected in a custom-made glass cell with a Bruker Vertex 70v FTIR spectrometer equipped with an MCT detector cooled with liquid nitrogen. A built-in gold mesh was used as counter electrode and a real RHE for reference.

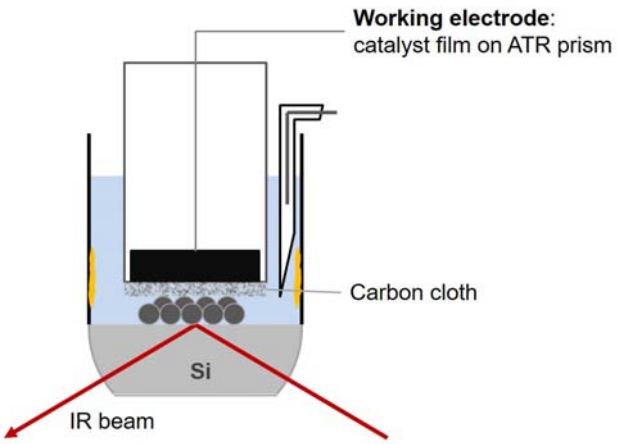

Figure S 7: Scheme of the *in situ* ATR electrochemical cell setup.

All *in situ* electrochemical measurements were controlled using a Metrohm Autolab PGSTAT204 potentiostat. An unpolarized beam was focused with a Pine Veemax II onto the sample spot of the

cell. The spectral resolution was set to 4 cm^{-1} and 128 interferograms were added together for each spectrum. Spectra are given in Reflectivity units defined as $\Delta R/R = R_{E2}-R_{E1}/R_{E1}$ with two single beam spectra R at applied potentials E_1 and E_2. Here the reference spectrum R_{E1} was collected in the same solution with 0.5 M EtOH and 0.1 M KOH immediately before the investigated potential scan at the respective start potential. A Si hemisphere was used as the IR window and an ink of the electrocatalyst sample (1 mg in 0.8 ml isopropanol and 0.2 ml milli-Q water) was deposited on the prism on the IR beam ATR focus spot and contacted with Toray Paper 060 carbon cloth and a Pine glassy carbon rod fixating the carbon cloth. The complete beam pathway was under vacuum more than 24 hours prior to each measurement.

Inductively coupled plasma- optical emission spectroscopy (ICP-OES) was used for compositional analysis, performed using a 715-ES-inductively coupled plasma analysis system (Varian). Standard concentrations were 2, 4.5 and 7.5 ppm for Pt and Ni and 0.7, 2.8 and 5.6 ppm for Rh. The chosen wavelengths for concentration determination were 203.646 nm, 214.424 nm, 265.495 nm and 306.471 nm for Pt; 216.555 nm, 221.648 nm, 222.295 nm, 222.486 nm, 227.021 nm, 230.299 nm and 231.604 nm for Ni and 233.477 nm, 246.103 nm, 249.078 nm, 343.488 nm and 369.236 nm for Rh. The error for the ICP measurements is at ± 1 wt%.

Transmission electron microscopy (TEM) was used to study nanoparticle morphology. A Cu grid (200 mesh) coated with a holey carbon film was impregnated with the sample solution and air-dried at 60 °C. An FEI TECNAI G² 20 S-TWIN microscope, equipped with a GATAN MS794 P CCD-detector operated at 200 kV was used. The mean particle size was determined from the TEM images by counting of at least 200 particles.

References

[1] S. C. S. Lai, M. T. M. Koper, *Physical Chemistry Chemical Physics* **2009**, *11*, 10446-10456.

[2] P. A. Christensen, S. W. M. Jones, A. Hamnett, *The Journal of Physical Chemistry C* **2012**, *116*, 24681-24689.

[3] aL. Vegard, *Zeitschrift für Physik* **1921**, *5*, 17-26; bL. Leppert, R. Q. Albuquerque, S. Kümmel, *Physical Review B* **2012**, *86*, 241403.

[4] M. Shao, J. H. Odell, S.-I. Choi, Y. Xia, *Electrochemistry Communications* **2013**, *31*, 46-48.

[5] N. Erini, S. Rudi, V. Beermann, P. Krause, R. Yang, Y. Huang, P. Strasser, *ChemElectroChem* **2015**, *2*, 903-908.